

Annual Report, 1999

3D Elastic Finite-Difference Simulation of a Dynamic Rupture (SCEC Group F)

Investigators: Dr. Kim B. Olsen,
Institute for Crustal Studies,
UC Santa Barbara

These results have been obtained in collaboration with Prof. Raul Madariaga and Sophie Peyrat (grad student), Ecole Normale Supérieure, Paris, Dr. Eiichi Fukuyama, NIED, Tsukuba, Japan, and Dr. Stefan Nielsen and Prof. Jean Carlson, UCSB.

Criticality of rupture dynamics in 3D

We have studied the propagation of seismic ruptures along a fault surface subject to a heterogeneous stress distribution and/or inhomogeneous frictional parameters. When prestress is uniform, rupture propagation is simple but presents some non-trivial differences with the circular shear crack models of Kostrov. The best known difference is that rupture can only start from a finite initial patch (or asperity). The other one is that rupture is not symmetric with the rupture front elongated in the inplane direction. Finally, if the initial stress is sufficiently high, the rupture front makes a transonic transition to super-shear speeds. For simple rectangular faults or asperities rupture propagation is clearly controlled by the width of the fault or asperity. When stress or strength are heterogeneous rupture propagation changes completely and is controlled by local length scales in the initial stress distribution as well as rupture resistance. Thus short rise times (Heaton pulses), rupture arrest, stopping phases, etc reflect the length scales of the stress and strength distribution. Through a number of numerical experiments we have identified a non-dimensional parameter that controls rupture. This parameter measures the ratio of local available strain energy to fracture energy derived from the friction law. A bifurcation occurs when this parameter is greater than a certain critical value that depends mildly on the geometry of the stress distribution on the fault (Fig. 1). We have verified that the non-dimensional parameter, computed using frictional parameters determined by different studies for several recent earthquakes (e.g., the 1992 Landers event) are near the critical value. Our results suggest that earthquakes are critical phenomena controlled by a single local non-dimensional number.

3D dynamic simulations of dipping faults: the Northridge earthquake

Here we use a mixed boundary condition which has been implemented in the 3D elastic finite-difference (FD) code in collaboration with Dr. Stefan Nielsen (Nielsen and Olsen, 2000). In this code we have implemented a dipping free-surface condition, which was used to simulate the 1994 Northridge earthquake. The prestress distribution is computed from the kinematic slip distribution by Wald et al. The simulations use a rate-and-state friction law, starting from a range of initial conditions of stress and frictional parameters. A critical balance between initial conditions and friction parameters has to be met in order to obtain a moment as well as a final slip distribution in agreement with kinematic slip inversion results. We find that the rupture process is strongly controlled by the average stress and connectivity of high-stress patches on the fault (Fig. 2). In particular, a strong connectivity of the high-stress patches is required in order to promote the rupture propagation from the initial nucleation to the remaining part of the fault. Moreover, we find that a small amount of rate-weakening is needed in order to obtain a level of inhomogeneity in the final slip similar to that obtained in the kinematic inversion results. However, when the amount of rate weakening is increased, the overall moment drops dramatically unless the average prestress is raised to unrealistic levels. A velocity-weakening distance on the order of a few centimeters per second is found to be adequate for an average prestress of about a hundred bars. The presence of the free surface and of the uppermost low-impedance layers in the model are found to have negligible influence on the rupture dynamics itself, because the top of the fault is at a depth of several kilometers. The 0.1-0.5 Hz radiated waves from the dynamic simulation provides a good fit to strong motion data at sites NWH and SSA. Underprediction of the recorded peak amplitude at JFP is likely due to omission of near-surface low velocity and 3D basin effects in the simulations.

The influence of friction and fault geometry on earthquake rupture

We investigate the impact of variations in the friction and geometry on models of fault dynamics. We focus primarily on a three dimensional continuum model with scalar displacements. Slip occurs on an embedded two dimensional planar interface. Friction is characterized by a two parameter rate and state law, incorporating a characteristic length for weakening, a characteristic time for healing, and a velocity

weakening steady state. As the friction parameters are varied there is a crossover from narrow, self-healing slip pulses, to crack-like solutions that heal in response to edge effects. For repeated ruptures the crack-like regime exhibits periodic or aperiodic systemwide events (Fig. 3). The self-healing regime exhibits dynamical complexity and a broad distribution of rupture areas. The behavior can also change from periodicity or quasi-periodicity to dynamical complexity as the total fault size or the length to width ratio is increased. Our results for the continuum model agree qualitatively with analogous results obtained for a one dimensional Burridge–Knopoff model in which radiation effects are approximated by viscous dissipation.

Dynamic modeling of the 1992 Landers, California, earthquake

We have modeled dynamic rupture propagation for the 1992 Landers earthquake using a fourth-order FD method (Olsen et al., 1997). In this method, the dynamic rupture grows spontaneously under the simultaneous control of the initial load and rupture resistance by friction, modeled using a simple slip weakening law. We used a simplified Landers fault model where the three segments were combined into one vertical, planar fault. By trial-and-error we modified the initial stress field until the dynamic rupture generated a rupture history and final slip distribution that approximately fit those determined by the kinematic inversions. We find that rupture propagation is extremely sensitive to small changes in the distribution of prestress and that energy release rate controls the average rupture speed. It is possible to control the rupture by maintaining a fixed initial stress field and modifying the rupture resistance locally. Clearly, dynamic models have many more degrees of freedom than kinematic inversions where the rupture velocity is typically heavily constrained. Our results suggest that, to some extent, the slip distribution and rupture velocity obtained by kinematic inversions reflect the initial stress distribution and rupture resistance, respectively. In order to validate our model we generated synthetic 0.5 Hz accelerograms from our dynamic simulation with a Green’s functions propagation (reflectivity) method. This method enables us to propagate the radiation generated by the dynamic rupture to distances greater than those feasible using the FD method. We find a satisfactory fit between our synthetics and the strong motion data (Fig. 4).

Analysis of dynamic rupture velocity

We have analysed variations in dynamic rupture propagation due to model features such as the free surface and fault width, and to rupture resistance on the fault. After an initial acceleration away from the nucleation, rupture slows down to about one half of the S-wave velocity upon reaching the boundaries of the fault (Fig. 5). When rupture has propagated about twice the distance from the nucleation to the fault boundary, the rupture velocity tends to increase, in part promoted by constructive interference by stopping phases from the fault boundaries. Here, three classes of rupture propagation are identified: the velocity (1) for the largest rupture resistance increase slowly towards the Rayleigh wave speed, (2) for intermediate rupture resistance repeatedly jump to super-shear values for a short distance but drop back to the Rayleigh wave speed, and (3) for the lowest rupture resistance jump to super-shear values and pertain values between the S- and P- wave velocities. The transitions between the three classes of rupture propagation are characterized by very narrow (critical) ranges of rupture resistance. The free surface promotes the generation of a head-wave (S^*), enabling rupture within class (1) to increase faster towards the Rayleigh wave velocity and periodically leap towards super-shear rupture velocity, and within (2) to permanently attain super-shear velocity. High-stress patches along the fault, with dimensions on the order of the fault width, promote two transitions to faster rupture velocities for class (1) ruptures: first to a value near the Rayleigh wave speed upon entering the high-stress area, and soon after to super-shear values. When reentering a low-stress area, the rupture velocity decreases to the sub-Rayleigh velocity.

Hybrid finite-difference and boundary integral element dynamic modeling

We have started to develop a hybrid method for flexible and efficient modeling of dynamic rupture propagation and its radiation in a heterogeneous three-dimensional medium. The dynamic rupture propagation is computed using the Boundary Integral Element (BIE) Method, which is capable of including faults

with non-planar geometries. However, the computation of radiated waves away from the fault becomes extremely expensive using the BIE method. Instead, we use an efficient fourth-order staggered-grid finite-difference (FD) method to model the dynamic radiation. The interaction between the two methods is implemented by extrapolating the particle velocities or stresses from the BIE dynamic rupture into the FD grid along a surface surrounding the fault, and by adding the radiation perturbation from the FD wave propagation to the fault plane used by the BIE method. The hybrid method enables dynamic modeling of rupture propagation on curved or multi-segmented faults in laterally and vertically heterogeneous earth models. The free-surface, which has been implemented in BIE methods only with limited accuracy, is included in the hybrid method with the same high accuracy as obtained in the FD grid. The main limitation of the method is that variation of the medium parameters on the fault is presently not possible. However, as the surface of interaction between the BIE and FD methods can be placed arbitrarily close to the fault, this limitation does not significantly affect the flexibility of the method.

References and SCEC publications

- Madariaga, R. and K.B. Olsen (2000). Earthquake dynamics, International handbook of seismology and physics of the earth's interior, Part II: theoretical seismology., Academic Press, submitted.
- Madariaga, R., and K.B. Olsen (2000). Criticality of rupture dynamics in 3D, submitted to *PAGEOPH*.
- Nielsen, S.B., and K.B. Olsen (2000). Constraints on stress and friction from dynamic rupture models of the 1994 Northridge, California, earthquake, submitted to *PAGEOPH*.
- Nielsen, S.B., J.M. Carlson, and K.B. Olsen (2000). The influence of friction and fault geometry on earthquake rupture, *Jour. Geophys. Res.*, accepted for publication.
- Olsen, K.B., R. Madariaga, and R.J. Archuleta (1997). Three-Dimensional dynamic simulation of the 1992 Landers Earthquake, *Science*, **278**, 834-838.
- Peyrat, S., K.B. Olsen, and R. Madariaga (1999). Dynamic modeling of the 1992 Landers, California, earthquake, *EOS AGU Fall Meeting*, 1999.

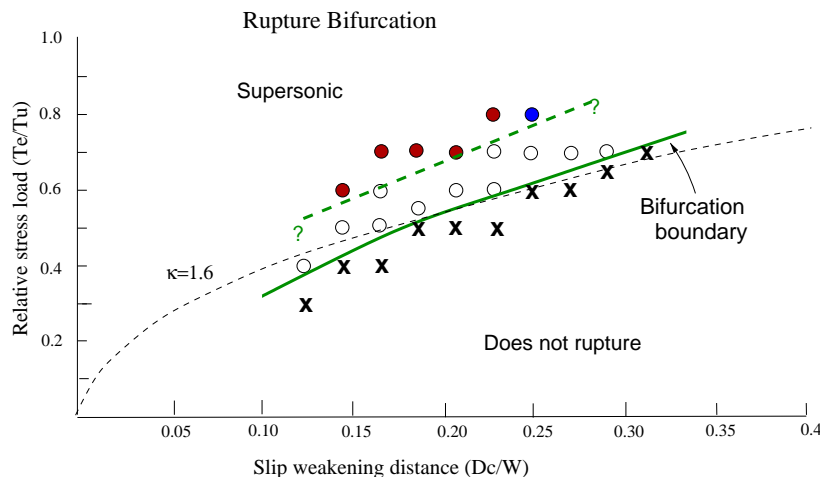


Figure 1: Bifurcation conditions for the growth of a rectangular fault. The crosses represent parameter values for which rupture stops spontaneously. The empty circles are parameter values for which rupture propagates along the fault with a rupture velocity below the shear wave speed. Filled circles are parameter combinations that produce super-shear fracture. The thick continuous and discontinuous lines separate these parameter fields. The thin dashed line is the approximate critical value $\kappa_c = 1.6$ and corresponds very well with the thick line, the critical boundary found experimentally.

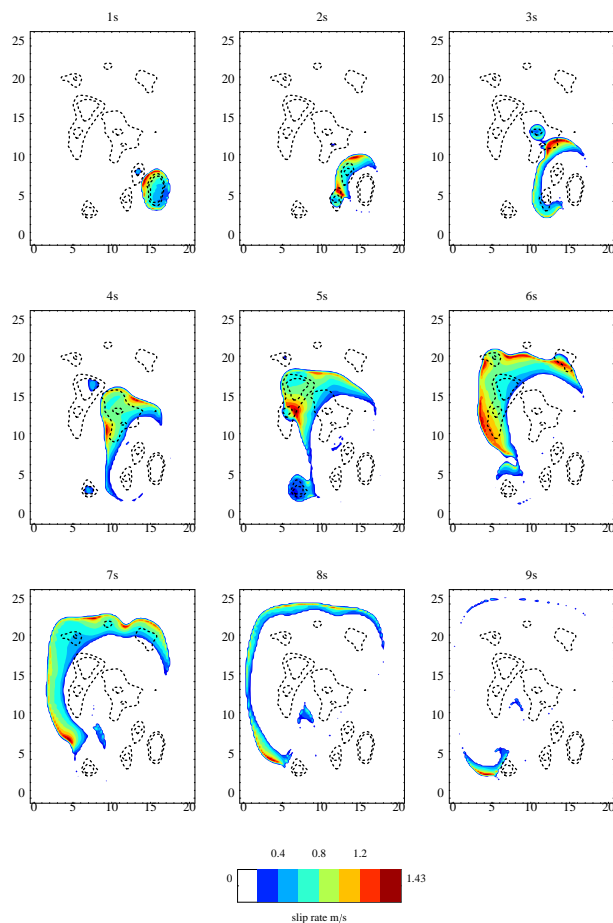


Figure 2: Snapshots of the sliprate for the dynamic simulation of the Northridge earthquake. The rupture follows a path between the patches of high stress, depicted by the dashed contours (150 and 170 bars).

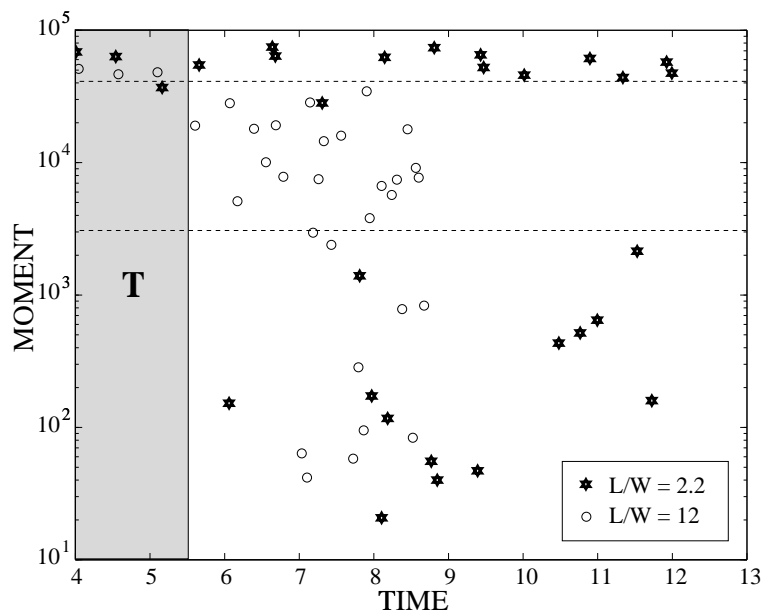


Figure 3: Moment release versus time for 30 repeated ruptures on faults with different aspect ratios. The stars correspond to the smaller aspect ratio $L/W = 2.2$, and the circles correspond to the larger aspect ratio $L/W = 12$. $L/W = 2.2$ produces aperiodic systemwide events, while $L/W = 12$ produces dynamical complexity, with a broad distribution of sizes of events. The grey shaded area marks the final stages of a transient regime where the fault is still influenced by an arbitrary imposed initial stress. The two horizontal dashed lines delimit an interval containing intermediate size events.

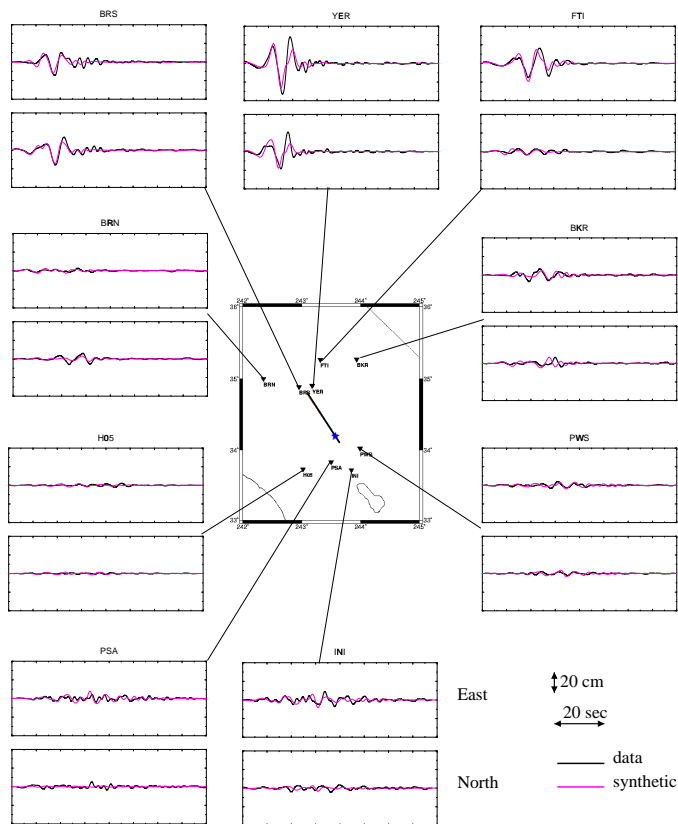


Figure 4: Comparison between dynamic radiation and strong motion data. The dynamic radiation is computed using a hybrid FD and reflectivity modeling method.

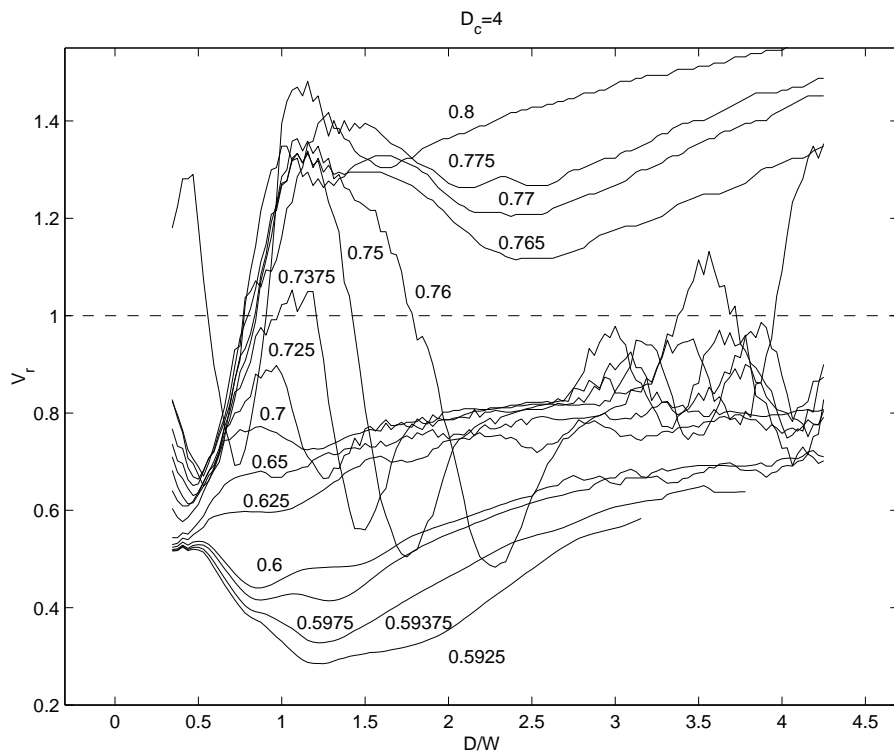


Figure 5: Rupture velocities along the in-plane direction from the nucleation, for a series of simulations with $D_c=4$ and T_e/T_u as indicated in the figure. The rupture velocities are computed using a 15-point average over time. The P and S wave velocities are superimposed for reference.